1995AJ....110..398S

THE PRECATACLYSMIC VARIABLE GD 245

GARY D. SCHMIDT, PAUL S. SMITH, AND DAVID A. HARVEY
Steward Observatory, University of Arizona, Tucson, Arizona 85721
Electronic mail: gschmidt@as.arizona.edu, psmith@as.arizona.edu, dharvey@as.arizona.edu

ALBERT D. GRAUER
Department of Physics & Astronomy, University of Arkansas at Little Rock, 2801 S. University, Little Rock, Arkansas 72204
Electronic mail: algrauer@ualr.edu

Received 1995 February 22; revised 1995 March 23

ABSTRACT

A combined photometric/spectroscopic study has been carried out of the evolved binary GD 245. The system is shown to consist of a DA2 white dwarf plus M3–5 secondary in a 4.17 h orbit. From model fitting to the white dwarf spectral features, the primary star is found to have $\log g = 7.77 \pm 0.02$ and $T_{\rm eff} = 22170$ K, leading to $M_1(g) = 0.48 \mathscr{M}_\odot$ and $R_1 = 0.0150 R_\odot$. Radial velocity analysis of the double-lined system implies $M_2 = 0.22 \mathscr{M}_\odot$. The distance is computed to be 61 pc and the orbital inclination is $i \approx 69°$. These parameters are consistent with the companion being a main-sequence object, in which case $T_{\rm eff} = 3560$ K, $R_2 = 0.27 R_\odot$, and the binary just escapes being an eclipsing system. A rich spectrum of emission lines phased in strength and radial velocity with the orbital motion is testimony to irradiation of a corotating secondary star by the white dwarf. However, the strength of this spectral component exceeds the intercepted Lyman continuum from the white dwarf, implying that alternate heating mechanisms are important. The companion underfills its Roche lobe by less than 25% in radius, and for current estimates of the angular momentum loss rate in close binaries will require less than 10^8 yr to evolve into contact. At the inception of mass transfer, the cataclysmic variable GD 245 will appear as one of the rare objects in the 2–3 h orbital period gap. © *1995 American Astronomical Society.*

1. INTRODUCTION

The list of short-period binaries containing one evolved component has grown considerably in recent years, due in large part to ground-based searches for companions to known compact objects (e.g., Saffer *et al.* 1993) and *EUV* surveys for recently formed stellar remnants (e.g., Thorstensen *et al.* 1995). The objects are important because they serve at once as a description of the outcome of common-envelope evolution and as a population of direct progenitors to the mass-transfer cataclysmic variables (CVs). In both stages of evolution, the physics of the star–star interaction is poorly understood, and each stands to benefit from firm observational constraints.

The presence of a companion to the bright white dwarf GD 245 (=EG232=WD2256+249=KUV2256+249; $V = 13.68$) has been realized by at least three groups in the past few years. Tytler & Rubenstein (1989) noted emission reversals in the Balmer lines and Schultz *et al.* (1993) inferred a close binary nature from rapid velocity variations in the emission lines. Our discovery was based on two optical spectra obtained in 1992 and 1993 as part of a spectropolarimetric survey for magnetic fields (Schmidt & Smith 1995) on white dwarfs selected from the McCook & Sion (1987) list. Those low-resolution (~7 Å) data revealed $\gtrsim 400$ km s^{-1} differences in the emission-line velocities between the two epochs and between the emission components and white dwarf absorption lines. For orbital motions in a white dwarf+late-type main-sequence binary, such variations can only occur for periods $P \lesssim 10$ h and rather high inclinations. Since the emission lines appear unresolved and TiO absorption bands are evident, it appeared that contact has not yet been established. Thus, the object was tentatively classified as a pre- or hibernating CV.

This paper reports followup photometry and echellette spectroscopy which confirm the binary nature of GD 245 and permit characterization of its stellar components. With an orbital period of 4.17 h, the object falls among the shortest period evolved binaries, and one for which information is already quite complete. If, as it appears, the secondary has a main-sequence structure appropriate for its mass, the star underfills its Roche lobe by $\lesssim 25\%$ in radius and will establish contact as an active CV in $< 10^8$ yr. A preliminary report of this work was presented by Schmidt *et al.* (1994).

2. OBSERVATIONS AND ANALYSIS

2.1 Photometry

Initial photometry of GD 245 was obtained on 1994 September 16 at the Center for Basement Astrophysics—West (NW Tucson) using a Celestron C-14 Schmidt–Cassegrain imaging onto an unfiltered, cooled TI 375×242 pixel CCD with 23×27 μm pixels at ~1.″5 pixel^{-1}. The S-BIG controller was programmed to read the CCD in consecutive 2 min exposures into a 486-based camera control computer. Subsequent data reduction was performed in IRAF on a SUN LX workstation. These data are included in the observational summary in Table 1 and a sample light curve is shown in Fig. 1 (*top*) as differential magnitudes relative to a comparison

 0004-6256/95/110(1)/398/7/$0.90 © 1995 Am. Astron. Soc.

© American Astronomical Society • Provided by the NASA Astrophysics Data System

1995AJ....110..398S

TABLE 1. Obervations.

Data Type	Date	Telescope	UT	$\lambda\lambda$ (Å)	$\Delta\lambda$ (Å)	Δt
Circular Spectropol.	1992 Oct. 23	2.3 m	6:57–7:06	4750–6660	7	10 min
Circular Spectropol.	1993 Oct. 8	2.3 m	6:47–6:54	4670–6790	7	8 min
Echellette Spectros.	1994 Aug. 1	2.3 m	7:05–11:09	3250–10500	2–4	12 min
Echellette Spectros.	1994 Sep. 8	2.3 m	4:57–10:56	3250–10500	2–4	12 min
CCD Photometry	1994 Sep. 16	CBA-W 14	5:15–9:42	~4000–8000	–	2 min
CCD Photometry	1994 Sep. 17	CBA-W 14	8:51–11:49	~4000–8000	–	2 min
CCD Photometry	1994 Sep. 23	CBA-W 14	3:23–9:57	~4000–8000	–	2 min
High-speed Photom.	1994 Oct. 10	1.5 m	3:23–10:21	*V*	–	10 s
High-speed Photom.	1994 Oct. 11	1.5 m	2:16–10:26	*B*	–	10 s
High-speed Photom.	1994 Oct. 12	1.5 m	2:53–9:05	*U*	–	10 s

star in the field of view. Evident here is a sinusoidal modulation of semiamplitude ~0.05 mag and period slightly longer than 4 h.

Absolute *UBV* photometry was added in 1994 October with the Lepus 3-channel system operating on the Mount Bigelow 1.55 m telescope of Steward Observatory. This instrument utilizes Hamamatsu R647-04 photomultiplier tubes in three identical photometers to record data from the program star, comparison star, and sky simultaneously. For these observations, the comparison star was located approximately 381″ E and 433″ N of the variable. Lepus also features continuous autoguiding on a third star to eliminate guiding errors. A 10 s integration time and Johnson *UBV* filters were employed throughout. At the beginning, during the course, and at the end of each time-series run the time base was calibrated to an accuracy of 0.1 s by visually comparing the time displayed on the data acquisition computer and the broadcast WWV time signals.

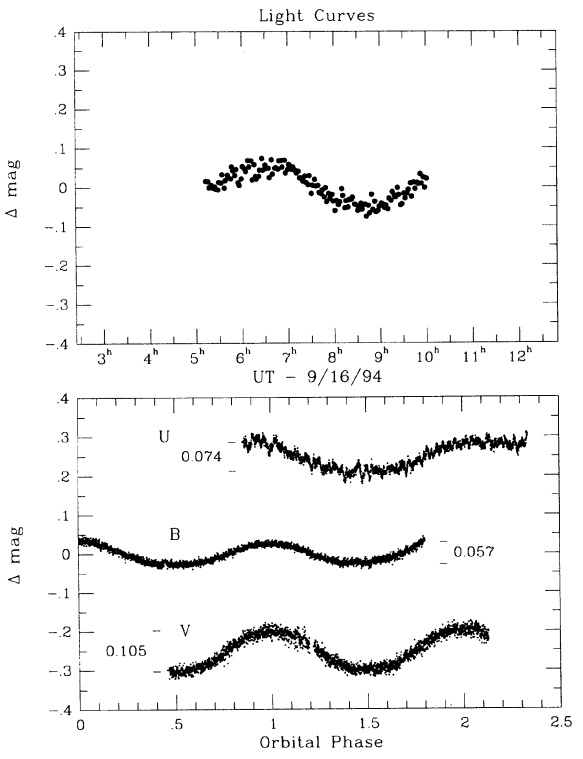

FIG. 1. Photometry of GD 245. (*Top*): Unfiltered photometry obtained with an S-BIG CCD camera and Celestron-14 telescope showing a smooth variation on a period slightly longer than 4 h. (*Bottom*): UBV measurements obtained on three consecutive nights with the Lepus 3-channel system and Bigelow 1.55 m telescope. The sinusoidal modulation is indicative of reprocessing of white dwarf emission by the orbiting secondary star. Full amplitudes of variation are noted and curves from successive filters are displaced by 0.25 mag for clarity. There is no evidence for eclipse or for flickering indicative of CV activity.

A relative gain ratio was constructed for the photometric channels by observing blank sky in all beams at the beginning of each time-series run. The sky-subtracted GD 245 data stream was then divided by the smoothed, sky-subtracted comparison star data, and a final correction was applied for differential extinction due to the color difference between the program and comparison stars. The resulting light curves are displayed in Fig. 1 (*bottom*), displaced by 0.25 mag between successive filters for clarity.

Standard stars (Landolt 1992) observed on two of the three nights allowed the photometry to be placed on the *UBV* system. With orbital phase registered to maximum light, the colors measured at φ=0.37 on October 10 were: V=13.73, $B-V$=−0.03, $U-B$=−0.88. Full amplitudes of modulation as determined from sinusoidal fits to the light curves are: ΔU=0.074, ΔB=0.057, ΔV=0.105.

The phasing of the light curves, whose maxima coincide with the emission-line brightness variations but are 90° out of phase with their radial velocities (Sec. *3.2*), is strong evidence that the continuum fluctuations arise through orbital motion of the (corotating) secondary, heated through the so-called reflection effect by the nearby white dwarf. Further support of this interpretation is provided by the red reprocessed spectrum, as indicated by the greater variation in the *V* vs *B* band. The intermediate *U*-band amplitude may reflect the importance of Balmer continuum emission from the companion star relative to the fainter white dwarf below the Balmer jump. The latter time series was also significantly affected by variable seeing, so the apparent flickering in this sequence should not be taken as evidence for CV activity. There is no indication in any of the light curves for an eclipse.

© American Astronomical Society • Provided by the NASA Astrophysics Data System

1995AJ....110..398S

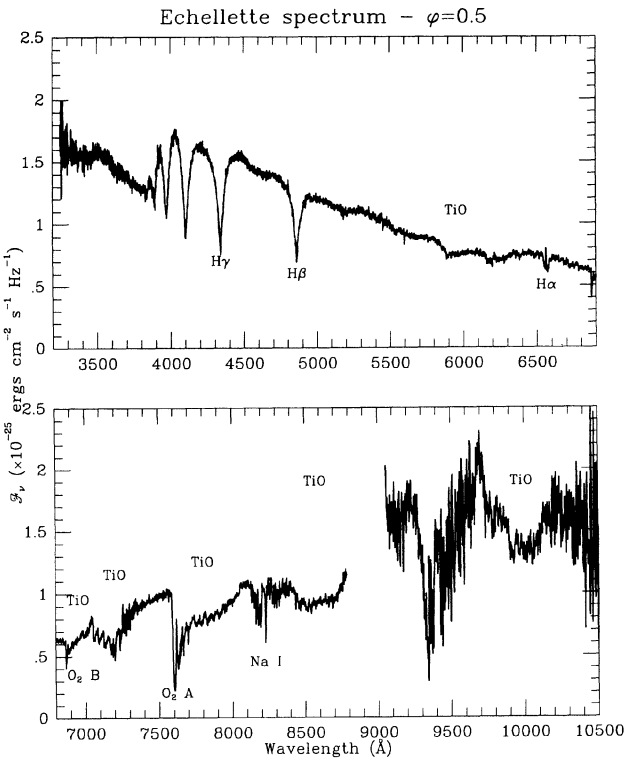

FIG. 2. Spectrum of GD 245 centered on minimum light. This composite from an echellette-format exposure represents inferior conjunction of the late-type companion star. The broad Balmer lines of the white dwarf primary are prominent in the top panel, while the longer wavelengths shown at the bottom are dominated by the TiO absorption spectrum of a late-type companion.

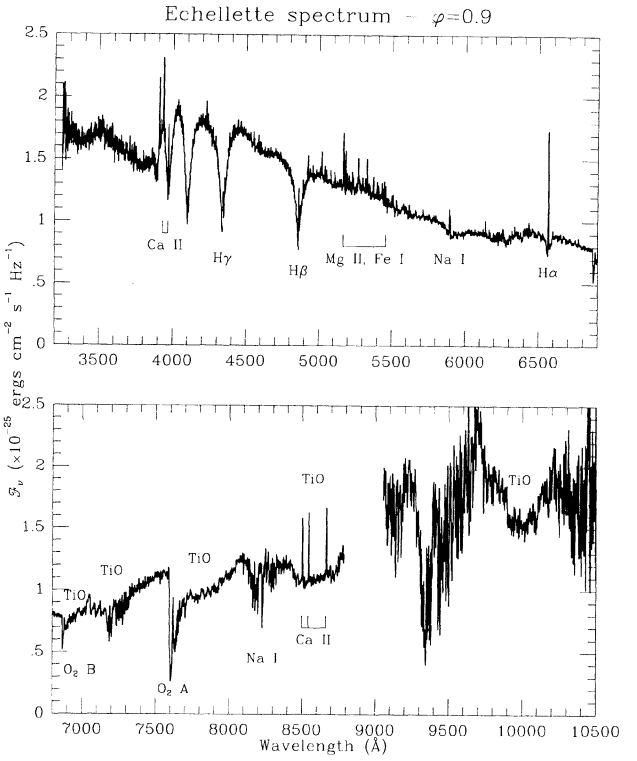

FIG. 3. As in Fig. 2 for a phase near maximum light. In this spectrum taken near superior conjunction, the heated photosphere of the secondary star is evident in the prominent emission-line spectrum of H, Ca II, Fe I, Mg II, and Na I. For the φ=0.9 orientation displayed, a significant velocity displacement of the Balmer emission reversals relative to the absorption features is apparent even at the scale of this figure. Instrumental resolution is ~150 km s^{-1} over the entire spectrum.

2.2 Echellette Spectroscopy

The echellette format of the 2.3 m Boller & Chivens spectrograph was chosen for dynamical study of the GD 245 binary because of its combination of high throughput, resolution, and very broad spectral coverage. When used with the facility 1200×800 15 μm square pixel Loral CCD, the 180 g mm^{-1} grating and 60° quartz cross-dispersing prism image the entire region λλ3250–10500 in 9 orders with only a small gap in the far red. A 2″×16″ slit provided resolution of ~150 km s^{-1} FWHM (2–4 Å for orders 12–4, respectively) and permitted adequate sky subtraction while separating the reddest orders. Spectral extraction and calibration were performed with the IRAF Echelle reduction package using exposures of a He–Ar comparison lamp and a flatfield source frequently interspersed in the time series. Spectral flux standards observed the same night enabled transformation to an absolute energy scale.

Two time series were obtained, in 1994 August and September (Table 1). We analyze the latter here because of its more extensive time coverage. Sample spectra compiled from two of the 12 min exposures are shown in Figs. 2 and 3, and represent approximately inferior and superior conjunction, respectively, of the companion star as computed from the ephemeris derived below. In assembling these composites, adjustments of 10%–20% had to be applied in order to match the flux levels of adjacent orders. This renders the overall energy distributions inadequate for accurate spectral deconvolution. However, Figs. 2 and 3 clearly display the blue continuum and broad absorption features of the white dwarf in the top panel plus a red, heavily blanketed component due to the late-type companion in the lower half. A rich emission-line spectrum due to H, Ca II, Fe I, Mg II, and Na I is prominent near phase 0.0. Essentially all of the structure in these spectra is real, with much of the hash beyond 9000 Å reflecting individual resolved H_2O absorption components in the terrestrial atmosphere.

3. SYSTEM PARAMETERS

3.1 Orbital Ephemeris

Compiling an initial ephemeris from the three consecutive nights of photometry in 1994 October was straightforward. The result was of sufficient quality to successfully predict the observed time of maximum light on September 23 to within 30 min, or 10% of a cycle. With this fiducial, all of the September–October photometry could then be phased. Relative to the latter ephemeris, the positive zero crossings of emission-line radial velocities from the August and September echellette runs occur at minimum light, consistent with both the variable continuum component and the emission lines arising on the heated inner hemisphere of the companion star. A common photometric/radial velocity ephemeris

© American Astronomical Society • Provided by the NASA Astrophysics Data System

1995AJ....110..398S

was then compiled. Expressed in terms of the heliocentric Julian date of maximum light, the final result is

$$\mathrm{HJD}_{\max}=2449627.0524(8)+0.173661(14)E,$$

where values in parentheses represent 1σ uncertainties for the last digits displayed. The orbital period of 4.1679 ±0.0003 h places GD 245 among other short-period evolved binaries and well within the domain of the CVs.

3.2 Stellar Components

Radial velocities are available for both stellar components from a host of emission and absorption lines contained in the echellette spectra. For the white dwarf, the most important are Hδ, Hγ, and Hβ. (Hα is too contaminated by the emission component at most phases to be useful.) Lorentzian profiles were fit to each line for the 24 consecutive exposures using a nonlinear least-squares technique adapted from Press *et al.* (1986). This permitted easy identification of emission features which contaminate the broad profiles (almost exclusively the Balmer reversals). The wavelength region containing each of these was then excised from the data and a second fit performed. Uncertainties in the velocity measurements were derived from the error matrix of the fit. These error bars are statistical in nature, and appropriate for velocity amplitude analysis. However, due to the modest density of He–Ar comparison lamp lines in these highly dispersed spectra, absolute (i.e., dc) velocities cannot be trusted to better than one-fifth of a resolution element, or ~30 km s^{-1}. We therefore do not quote a systemic velocity for the binary. The semiamplitudes computed from least-squares fits to a sine wave for the three white dwarf absorption features expressed in km s^{-1} are: Hδ: 90±9; Hγ: 112±9; Hβ: 95 ±15, for a mean of $K_1=101\pm6$ km s^{-1}.

The motion of the secondary can be tracked through the prominent emission reversals of Hβ and Hα, using as input the residuals from the fits to the white dwarf lines described above. These measurements display velocity curves which are antiphased with the white dwarf curves, confirming an origin on the companion star. To test for the importance of biasing by the fact that irradiation is confined to the inner hemisphere of the star, the location of the λ7054 (0-0) TiO absorption bandhead was also measured for each exposure. The semiamplitudes computed for these three features are: Hβ: 215±19; Hα: 212±6; TiO: 222±7 km s^{-1}. The effect is marginal, if real. Because irradiation tends to weaken the M-star absorption features while giving rise to the emission lines (Wade & Horne 1988, cf. also Figs. 2 and 3), the biases will tend to offset in an average of the two types of measurement. We therefore quote the mean of $K_2=216\pm4$ km s^{-1} for the velocity semiamplitude of the secondary star. The individual measurements are compared to fitted sinusoids for both stars in the upper two panels of Fig. 4.

Finally, in the bottom panel of Fig. 4 is displayed the flux in the Hα reversal versus orbital phase. This measure of emission-line strength shows the smooth, sinusoidal dependence characteristic of reprocessing by the secondary. As is evident from comparison of the spectra in Figs. 2 and 3, this behavior is shared by all of the emission lines. The disappearance of Ca II features around $\varphi=0.5$ is particularly strong evidence that any intrinsic chromospheric activity of the secondary is minor in comparison with that due to irradiation. There is a hint that maximum line strength may be displaced by $\Delta\varphi\sim-0.05$ from the expected peak at superior conjunction. Since the ephemeris is referenced to the broadband photometry as well as the radial velocity variations, this shift, if real, would imply that the region of the secondary which produces the line emission is offset from that responsible for the reprocessed continuum. Our opinion is that one must be cautious not to overinterpret photometry obtained at the slit of a spectrograph.

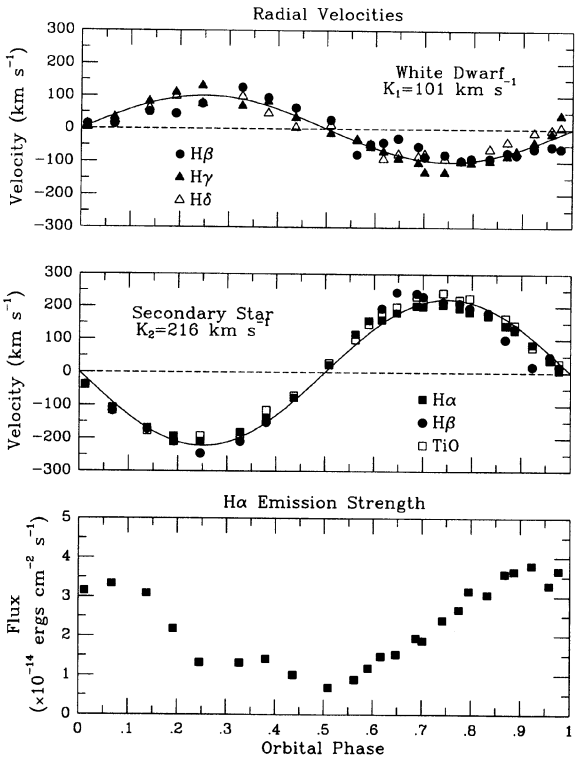

FIG. 4. Stellar radial velocity curves and a measure of emission-line strength. *Top*: Displacements of the Hδ, Hγ, and Hβ absorption lines of the white dwarf compared with the best-fit sinusoid for the common photometric/spectroscopic period. *Middle*: Velocity measurements for the emission reversals of Hβ and Hα compared with the prominent λ7054 TiO absorption bandhead and the fitted sine curve representing the motion of the secondary star. The ratio of velocity amplitudes implies a mass ratio $q=\mathcal{M}_1/\mathcal{M}_2=2.15\pm0.13$. *Bottom*: Flux in the Hα emission reversal plotted vs orbital phase.

The coadded spectrum of the region Hβ–H9 centered around minimum light was kindly analyzed by P. Bergeron (private communication) for the temperature and surface gravity of the primary star. The $M(g)$ technique used involves a comparison of the observed line profiles with the predictions of an accurate grid of stellar models, and is particularly effective when applied to DA white dwarfs of moderate temperature (Bergeron, *et al.* 1992). A mass is then available from a mass–radius relation for white dwarfs. For GD 245, the line-profile analysis yields $\log g=7.77\pm0.02$,

© American Astronomical Society • Provided by the NASA Astrophysics Data System

1995AJ....110..398S

TABLE 2. GD 245 system parameters.

Property	Primary	Secondary
K (km s^{-1})	101 ± 6	216 ± 4
$\log g$	7.77 ± 0.02	...
Mass ($M_\odot$)	0.48 ± 0.02	0.22 ± 0.02
Radius ($R_\odot$)	0.0150 ± 0.0005	0.27 ± 0.02 (MS)
$T_{\rm eff}$ (K)	22170 ± 130	3560 (MS)
Spectral Type	DA2	M3 – 5 (M3.5 MS)
Period	4.1679 ± 0.0003 hr	
Semimajor axis	$1.17 \pm 0.01\ R_\odot$	
Distance	61 ± 2 pc	
Inclination	$69^{\circ}{}^{+8}_{-7}$	

$T_{\rm eff}$=22170±130 K.[1] Error bars here are formal uncertainties of the fit. Like all such estimates, the measurements may be subject to additional errors due to the unknown composition of the core (C or He), inaccuracy of the models, etc. At these moderate temperatures, however, such uncertainties are likely to be minor. Using the evolutionary models of Wood (1990; see also Bergeron *et al.* 1992), the implied mass is $\mathcal{M}_1(g)=0.48\pm0.02\mathcal{M}_\odot$ for a thin surface layer of hydrogen; $0.51\pm0.02\mathcal{M}_\odot$ for a thick ($10^{-4}\mathcal{M}_\odot$) hydrogen layer. We adopt the former value. With a mass ratio $q=\mathcal{M}_1/\mathcal{M}_2=2.15\pm0.13$ from the radial velocity analysis, the secondary therefore has a mass $\mathcal{M}_2=0.22\pm0.02\mathcal{M}_\odot$.

We have compared the red absorption spectrum of GD 245 with the atlas of M dwarf spectra compiled by Kirkpatrick *et al.* (1991). For wavelengths shortward of 9000 Å, the features best match template stars in the interval M3–5, with the rather large range due to uncertainty in the strength of the underlying white dwarf component and the adjustments which had to be made to match flux levels of adjacent orders. Longer wavelengths show that the TiO/FeH feature at 1 μm is stronger than normal for these spectral types (Kirkpatrick *et al.* 1993). The technique of Wade & Horne (1988), which is based on the relative flux deficits in the λ7165 and λ7665 TiO bands, is complicated by the fact that the two features occur in different orders of our echellette spectrum. Nevertheless, the estimate of M4.5 (±~0.5) for the minimum-light orientation is broadly consistent with the main-sequence interval for the allowed mass range: M3.2–3.7 (Kirkpatrick & McCarthy 1994), in which case the surface temperature is near $T_{\rm eff}$ (MS)=3560 K. The empirical mass–radius relation for low-mass stars preferred by Patterson (1984), $R\propto\mathcal{M}^{0.88}$, then suggests a radius of R_2 (MS)=$0.27\pm0.02R_\odot$. These and other pertinent parameters of the GD 245 system are summarized in Table 2.

For the inferred effective temperature and radius, the white dwarf has an absolute B-band magnitude of +9.83. Estimating 5%–10% contamination by the companion in this waveband, the absolute photometry implies a distance of 61±2 pc. Again using the calibration of Kirkpatrick & McCarthy (1994), a companion star of main-sequence spectral type M3.5 at this distance will have an apparent brightness of 3.3×10^{-26} ergs cm^{-2} s^{-1} Hz^{-1} at R and 1.1×10^{-25} ergs cm^{-2} s^{-1} Hz^{-1} at I. By comparison with the measured flux levels (Figs. 2 and 3), these predictions appear reasonable, as they imply that the white dwarf provides ~55% and ~30% of the light at the two wavelengths, respectively.

The reprocessing scenario can be tested by comparing the observed Hα flux with what is expected for irradiation by the white dwarf. For the parameters in Table 2 and the pure-H, unblanketed model energy distributions of Wesemael *et al.* (1980), the Lyman-continuum photon flux onto the companion's surface is $N_{\rm ion}\sim4\times10^{16}$ cm^{-2} s^{-1}. Assuming at most one Hα photon per incident ionizing photon and reradiation into 2π str results in a maximum reprocessed Hα flux at the Earth of $F_{\rm H\alpha}\sim6\times10^{-16}$ ergs cm^{-2} s^{-1}. This is to be compared with the value of 3.7×10^{-14} ergs cm^{-2} s^{-1} measured when the companion is nearly face on (φ=0). The ionizing radiation field from the white dwarf thus falls far short of that required to power the line emission from the secondary. This has been a problem in the past: Saffer *et al.* (1993) appealed to intrinsic (dMe) activity in PG1026+002, which also contains a rather cool ($T_{\rm eff}\sim17600$ K) white dwarf. The near disappearance of all emission lines at inferior conjunction makes that explanation very unsatisfactory for GD 245. Moreover, the discrepancy is so large that a stellar radius would have to be increased by a factor of 8, the distance decreased to less than 10 pc, or the temperature of the white dwarf doubled to bring them into even marginal agreement. We suggest instead that photoionization from n=2 should be considered. The Balmer continuum of a white dwarf in this temperature regime provides ample photons, and the incident radiation field might be sufficiently strong that sources of opacity which usually dominate the near UV in an M-star atmosphere—molecules and neutral atoms—would be greatly diminished. Indeed, GD 245 would seem to provide an excellent laboratory for studying surface heating of stars.

The strong modulation of Hα emission flux in Fig. 4 (semiamplitude ~70%) is one indication of high orbital inclination. Following the treatment in Thorstensen *et al.* (1978), we would conclude that i>45°, depending on the amount of line emission intrinsic to the star (i.e., not due to heating). A firmer estimate results from a comparison of the measured velocity amplitudes with the implied orbital motions for the derived period and masses. This yields $i=69^{\circ}{}^{+8}_{-7}$. Again, the result is consistent with the presence of a main-sequence secondary, in which case the absence of primary eclipse requires i<77°. Apparently, GD 245 just escapes being an eclipsing system.

3.3 Proximity to Contact

For the stellar masses and period derived above, the semimajor axis of the GD 245 binary is $a=1.17\pm0.01R_\odot$. In a coordinate system in which the x axis is directed along the line of centers and z is parallel to the orbital axis, the dimensions of the corresponding Roche surface surrounding the secondary are: $X_2=0.49R_\odot$; $Y_2\approx Z_2=0.35R_\odot$ (e.g., Pringle & Wade 1985). A main-sequence star of the indicated mass would therefore fit within the surface. Absence of con-

[1]The spectral type of DA4 listed by McCook & Sion (1987) was apparently based on $B-V$ colors, which are contaminated by the secondary. Based on the new analysis, DA2 is a better estimate.

© American Astronomical Society • Provided by the NASA Astrophysics Data System

1995AJ....110..398S

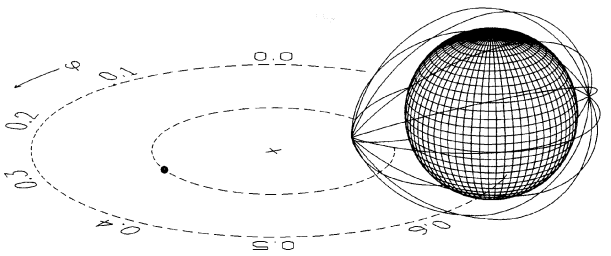

FIG. 5. Scale drawing of the GD 245 binary and secondary Roche surface for orbital phase φ=0.84 and the system parameters derived in the text. Phase is registered to maximum light, when the reprocessing surface of the companion is viewed most directly. From the Earth's perspective, the binary just misses being an eclipsing system.

tact is consistent with our spectroscopy, which reveals all emission lines to be single component, have widths $\Delta v \lesssim 150$ km s^{-1}, and display radial velocities and strengths appropriate for an origin solely on the inner hemisphere of the secondary. However, the star would have rather little breathing room, as it underfills the lobe by less than 25% in the y and z directions. A scale drawing of the binary and secondary Roche surface as viewed from Earth is provided as Fig. 5.

The time until the secondary contacts its Roche lobe can be estimated assuming an angular momentum loss rate. Gravitational radiation alone would require $t_{GR} > 2\times10^9$ yr to initiate mass transfer. Braking through a magnetically channeled wind—as is invoked to explain the rotation rates of low mass main-sequence stars—is generally assumed to apply also to the late-type secondaries of CVs. Explanations of the 2–3 h CV period gap have traditionally relied on a cessation of magnetic braking at a specific secondary mass ($\mathcal{M} \sim 0.2 \mathcal{M}_\odot$). However, *ROSAT* has found no evidence that stellar activity suddenly diminishes for very late spectral types (Fleming *et al.* 1993). If magnetic braking or a similarly lossy mechanism operates for secondaries as small as the $0.22 \mathcal{M}_\odot$ star in GD 245, the time to contact could be substantially reduced. For example, the braking rates of Verbunt & Zwann (1981; see Ritter 1986) imply that mass transfer would commence in $t_{MB} < 10^8$ yr.

At $T_{\rm eff} \sim 22000$ K, the age of the white dwarf is $\lesssim 10^8$ yr (e.g., Wood 1990). While not as young as some of the pre-CVs being found in *EUV* surveys, rather little period evolution can have taken place. GD 245 must have emerged from the common envelope already as a short-period system ($P < 6$ h). In the list of de Kool & Ritter (1993), only MT Ser (sdO+M), HW Vir (sdB+?), and NN Ser (DAO+M5-6) have orbital periods which are shorter.[2] Because of its brightness and comparable contributions from the two stellar components, GD 245 is an ideal candidate for study and has already yielded the best-determined orbital and stellar parameters.

All available data suggest that GD 245 harbors an unevolved secondary of main-sequence characteristics. It is therefore likely that the system represents a pre-CV as opposed to a previously interacting system currently in hibernation (e.g., Shara 1989). With the orbital period scaling as the $\frac{3}{2}$ power of separation from Kepler's third law, the period upon contact will be $P_c \sim 2.7$ h, so GD 245 will first appear as a CV as one of the rare objects in the 2–3 h gap. Traditionally, the gap has been linked to the onset of core convection in the secondary, which is thought to disrupt the dominant (magnetic) braking mechanism near $P = 3$ h and allow the slightly out-of-equilibrium star to shrink back within its Roche lobe. Mass transfer is not reestablished until residual braking mechanisms (e.g., gravitational radiation) return the two to contact near the lower edge of the gap. Of the objects whose periods have been found to lie in the 2–3 h range, more than one-half are AM Her systems, even though these magnetic binaries comprise a clear minority of all CVs. One possible explanation for this observation is that the strong magnetic field on an AM Her primary somehow removes the braking discontinuity required to initiate the gap (e.g., King 1993). For the case at hand, the primary is distinctly *non*-magnetic ($B_e < 21$ kG; $\mu \lesssim 2\times10^{31}$ G cm^3; Schmidt & Smith 1995). When GD 245 appears in the gap, it will do so by being born there.

We are pleased to thank J. Waack of the Telescope Operations Group for assistance with assembly of the echellette optics, M. Lesser and the Steward CCD Group for the outstanding detector operating on this instrument, and P. Bergeron for model fitting of the white dwarf spectrum. Thanks also go to J. Liebert for a critical reading of an earlier version of the manuscript, and to the referee, R. Saffer, for several helpful suggestions. Lowell Observatory provided hospitality and scientific support to G.D.S. while this paper was being written. Financial support was obtained from the National Science Foundation through Grant Nos. AST 91-14087 (G.D.S.), AST 88-13572 and AST 90-13368 (A.D.G.), and from NASA through Grant No. NAG 5-1630 (P.S.S.).

[2]There is certainly a bias against discovering precataclysmic binaries in which the white dwarf is too cool to significantly heat the companion. The lack of highly evolved primaries among the shortest-period detached systems may also reflect the rapid period evolution of close binaries, which for typical mass ratios and initial periods $P < 3$ h initiates mass transfer on a time scale similar to the stellar evolution time from common envelope to white dwarf phase.

REFERENCES

Bergeron, P., Saffer, R. A., & Liebert, J. 1992, ApJ, 394, 228
de Kool, M., & Ritter, H. 1993, A&A, 267, 397
Fleming, T., Giampapa, M., Schmitt, J., & Bookbinder, J. 1993, ApJ, 410, 387
King, A. R. 1993, in Interacting Binary Stars, edited by A. Shafter (ASP, San Francisco), p. 189
Kirkpatrick, J. D., Henry, T. J., & McCarthy, D. W. 1991, ApJS, 77, 417
Kirkpatrick, J. D., Kelly, D. M., Rieke, G. H., Liebert, J., Allard, F., & Wehrse, R. 1993, ApJ, 402, 643
Kirkpatrick, J. D., & McCarthy, D. W. 1994, AJ, 107, 333
Landolt, A. U. 1992, AJ, 104, 340
McCook, G. P., & Sion, E. M. 1987, ApJS, 65, 603

© American Astronomical Society • Provided by the NASA Astrophysics Data System

1995AJ....110..398S

Patterson, J. 1984, ApJS, 54, 443
Press, W. H., Flannery, B. P., Teukolsky, S. A., & Vetterling, W. T. 1986, Numerical Recipes (Cambridge University Press, Cambridge)
Pringle, J. E., & Wade, R. A. ed. 1985, Interacting Binary Stars (Cambridge University Press, Cambridge), Appendix
Ritter, H. 1986, A&A, 169, 139
Saffer, R. A., *et al.* AJ, 105, 1945
Schmidt, G. D., & Smith, P. S. 1995, ApJ (in press).
Schmidt, G. D., Smith, P. S., Harvey, D. A., & Grauer, A. G. 1994, BAAS, 26, 1344
Schultz, G., Zuckerman, B., & Becklin, E. E. 1993, BAAS, 25, 824
Shara, M. M. 1989, PASP, 101, 5
Thorstensen, J. R., Charles, P. A., Margon, B., & Bowyer, S. 1978, ApJ, 223, 260
Thorstensen, J. R., Vennes, S., & Shambrook, A. 1994, AJ, 108, 1924
Tytler, D., & Rubenstein, E. 1989, in White Dwarfs, IAU Colloquium No. 114, edited by G. Wegner, (Springer, Berlin), p. 524
Verbunt, F., & Zwann, C. 1981, A&A, 100, L7
Wade, R. A., & Horne, K. 1988, ApJ, 324, 411
Wesemael, F., Auer, L. H., Van Horn, H. M., & Savedoff, M. P. 1980, ApJS, 43, 159
Wood, M. 1990, Ph.D. thesis, University of Texas at Austin

© American Astronomical Society • Provided by the NASA Astrophysics Data System